Modeling Neutral Particle Flux in High Aspect Ratio Holes using a One-Dimensional Radiosity Approach

Paul Manstetten*, Lado Filipovic+, Andreas Hössinger#, Josef Weinbub*, Siegfried Selberherr+
*Christian Doppler Laboratory for High Performance TCAD at the
+Institute for Microelectronics, TU Wien, Gußhausstraße 27-29, 1040 Wien, Austria
#Silvaco Europe Ltd., Compass Point, St Ives, Cambridge, PE27 5JL, United Kingdom
Email: manstetten@iue.tuwien.ac.at

1. Introduction

We propose a one-dimensional radiosity model to approximate the local flux on the wall and bottom of high aspect ratio (HAR) holes during three-dimensional plasma etching simulations. In this work we consider an ideal cylindrical shape, ideal diffuse reflections/sources, and a sticking probability *s*, independent of the flux; ballistic transport is assumed for the neutral particles.

The diffuse re-emission mechanism is a common assumption for neutral particles [1] and cylinder-like shapes are a key prerequisite for HAR holes in the context of, for instance, 3D NAND processing [2].

During a plasma etching simulation the local fluxes of the etching species are used to model the surface reactions. The local flux must be recalculated for each simulation time step, because the interface positions are changing due to the evolving surface. For HAR features, the local flux originating from re-emission is prominent and the local flux rates can easily vary by orders of magnitude along the feature depth.

Considering the computational costs of a three-dimensional plasma etching simulation, the calculation of the local flux is dominant. The efficient calculation of the neutral flux is therefore essential considering especially the fact that HARs further increase this dominance.

Common approaches for three-dimensional flux calculation are Monte Carlo ray tracing [3] and radiosity based [4] methods. Ray tracing supports bi-directional reflectance distribution functions, whereas radiosity inherently favors diffusely reflecting surfaces.

We propose a computationally inexpensive one-dimensional approach, which reproduces the results obtained by a three-dimensional ray tracing simulation, and can therefore be used as a drop-in replacement for cylinder-like hole structures.

2. One-Dimensional Radiosity

The simulation domain (Fig. 1) is a circular cylinder parameterized along its depth and radius. We model the source of neutral particles by an ideal diffusely-emitting disk closing the cylinder at the top without re-emission ($s=1$). The wall of the cylinder is an ideal diffuse reflector with a constant sticking probability ($s=s_w$). The bottom of the cylinder does not have any re-emission ($s=1$). This setup is a reasonable approximation for the neutral flux in a HAR plasma etching environment.

Our approach is based on rotational symmetry and a subdivision of the cylinder into surface elements (Fig. 1). By assuming a constant flux and a constant sticking probability over each surface element, the problem can be formulated using the discrete radiosity equation: For a surface element *i* the equation reads

$$B_i = E_i + (1-\alpha_i)\cdot\sum_j (F_{j\to i}\cdot B_j)\ , \qquad (1)$$

where *B* is the radiosity (sum of emitted and reflected energy), *E* is the emitted energy, α is the absorptance and $F_{j\to i}$ is the view factor (proportion of the radiated energy which leaves element *j* and is received by element *i*). The radiosity *B* is related to the absorbed energy *A* by

$$A_i = (B_i - E_i)\cdot\alpha_i/(1-\alpha_i)\,. \qquad (2)$$

We adapt Equation (2) to our problem by substituting the absorbed energy *A* by the flux and the absorptance α by the sticking probability *s*. The view factors *F* are derived using an analytical formula for two coaxial disks of unequal radius [5].

The solution to the resulting diagonally-dominant linear system of equations is approximated with the Jacobi method.

3. Results

The normalized flux distributions for holes with aspect ratios (ARs) 5 and 45 are shown in Fig. 2. The non-continuity of the sticking probability causes a jump at the wall-bottom interface. The flux is normalized to the flux on a surface fully exposed to an infinite source plane. Fig. 3 and Fig. 4 compare the flux distributions for $AR=5$ obtained using the proposed one-dimensional radiosity approach with results generated by a reference Monte Carlo ray tracing tool [6]; similarly, Fig. 5 and Fig. 6. compare the flux distributions for $AR=45$.

The results show a good agreement, beside the deviation at the wall-bottom interface, caused by the discretization which is used in the ray tracing simulation. The separation of the flux distributions, particularly visible for $s_w=0.2$ (Fig. 5), and the visible noise in Fig. 6, reflect the stochastic nature of the ray tracing approach.

4. Summary

We provide an approximation of the local neutral flux in three-dimensional plasma etching simulations of HAR holes using a one-dimensional radiosity approach. Comparing the results with a three-dimensional Monte Carlo ray tracing simulation shows good agreement.

The financial support by the *Austrian Federal Ministry of Science, Research and Economy* and the *National Foundation for Research, Technology and Development* is gratefully acknowledged.

References

[1] A. Kokkoris et al., Vacuum Sci. & Techn. **A 24** (2006).
[2] H.-T. Lue, Charge-Trapping Non-Volatile Mem. (2015).
[3] O. Ertl et al., Microelectronics Eng. **87** (2010).
[4] T. Ikeda et al., Proc. of SISPAD. (2011).
[5] M. Modest et al., Radiative Heat Transfer. (2013).
[6] ViennaTS, https://github.com/viennats/.

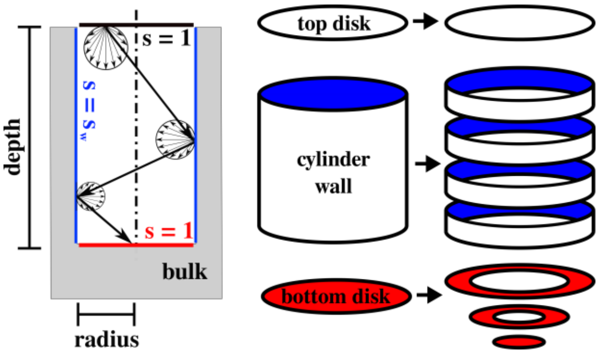

Fig. 1: *Left:* The simulation domain is decomposed into a fully adsorbing source (black), a partly adsorbing wall (blue) and a fully adsorbing bottom (red). *Right:* The wall and bottom are subdivided into ring elements; the top disk is not subdivided as the flux distribution leaving the cylinder is not of relevance.

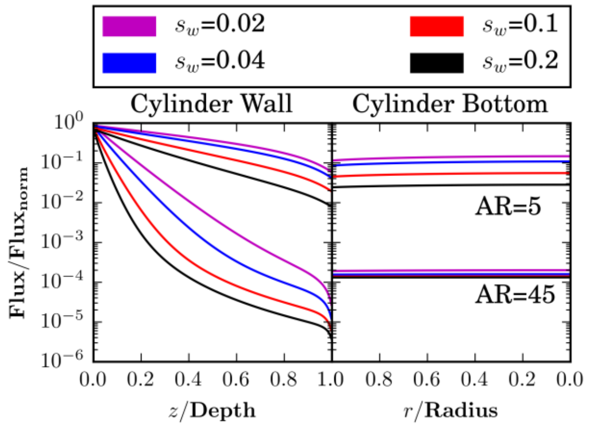

Fig. 2: *One-Dimensional Radiosity:* Normalized flux distribution along the wall (left) and the bottom (right) of holes with aspect ratios *AR=5* (upper group) and *AR=45* (lower group). The sticking probability of the wall s_w is varied from *0.02* to *0.2*.

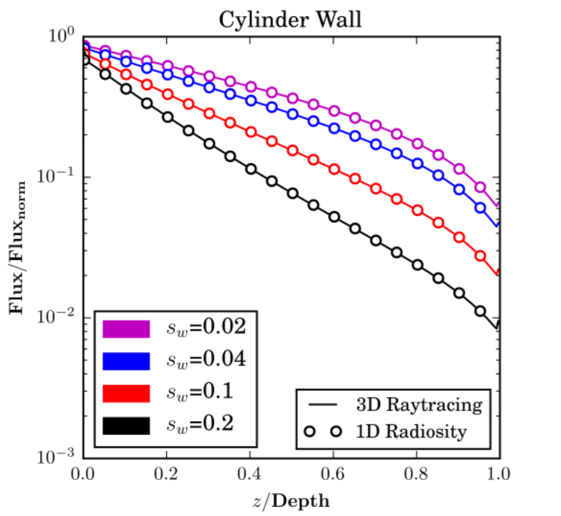

Fig. 3: *Ray Tracing vs. Radiosity (AR=5):* Flux along the wall for different sticking probabilities s_w. The ray tracing results show an increasing flux near the wall-bottom interface.

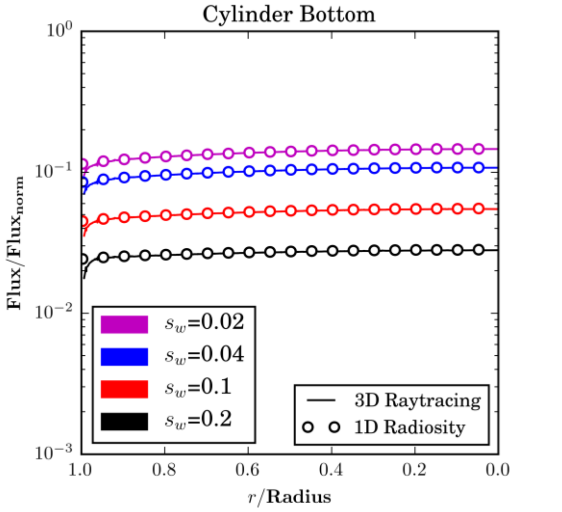

Fig. 4: *Ray Tracing vs. Radiosity (AR=5):* Flux along the bottom for different sticking probabilities s_w. Differences are visible near the wall-bottom interface.

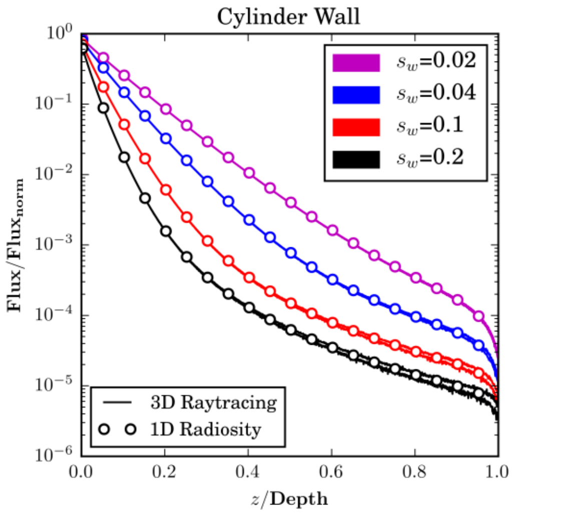

Fig. 5: *Ray Tracing vs. Radiosity (AR=45):* Flux along the wall for different sticking probabilities s_w. For each depth, minimum and maximum are plotted for the ray tracing results; the difference increases towards the bottom interface.

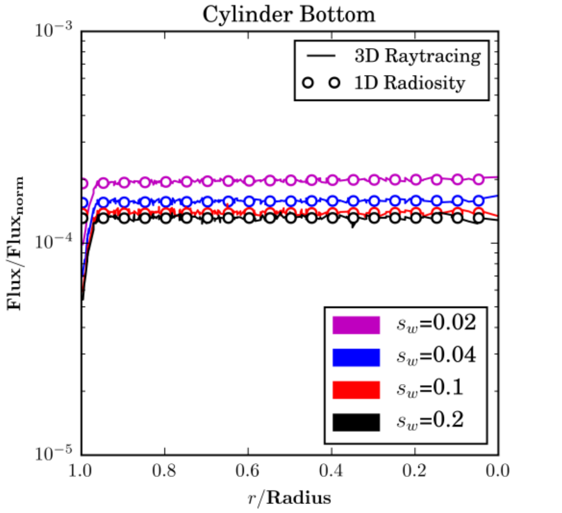

Fig. 6: *Ray Tracing vs. Radiosity (AR=45):* Flux along the bottom for different sticking probabilities s_w. Differences are visible near the wall-bottom interface. The ray tracing results reveal noise over the entire domain.